COMMUNICATION

Check for updates

Interplay between connectivity and passivating agents in perovskite quantum dot networks†

María Morán-Pedroso,‡ David O. Tiede,‡ Carlos Romero-Pérez,
Mauricio E. Calvo, [ID] Juan F. Galisteo-López [ID] * and Hernán Míguez [ID] *

Introducing quantum dots (QDs) as the active element of an optoelectronic device demands its incorporation in the shape of interconnected arrays that allow for some degree of electronic coupling in order to inject/extract charge carriers. In doing so, beyond reducing the degree of quantum confinement, carriers are exposed to an enhanced defect landscape as they can access adjacent QDs, which is at the origin of the strong reduction of photoluminescence observed in QD solids when compared to that of the isolated QDs. In this work we demonstrate how a proper defect passivating strategy or atmospheric treatment can greatly enhance charge diffusion in a QD film, needed for an optimal carrier injection/extraction demanded for optoelectronic applications, and also improved its stability against external radiation. From a fundamental perspective, we provide evidence showing that trap density distribution, rather than QD size distribution, is mostly responsible for the observed variations in emission decay rates present in the QD networks under analysis.

1. Introduction

Over the past decade, halide perovskites (HPs) have emerged as a family of semiconductors with potential for applications in diverse fields from photovoltaics,[1] light emission,[2,3] photocatalysis[4] or radiation detection[5] having achieved state-of-the-art performances in many cases. An appropriate choice of precursors allows for attaining conventional three-dimensional (3D) perovskites having the chemical formula ABX_3 (with A being a monovalent cation, B a bivalent metallic cation and X a halide anion), low-dimensional structures comprising n-dimensional inorganic films separated by large organic molecules[6] or other structures such as double

Instituto de Ciencias de Materiales de Sevilla (Consejo Superior de Investigaciones Científicas-Universidad de Sevilla), C/Américo Vespucio, 49, Sevilla, 41092, Spain. E-mail: juan.galisteo@csic.es, h.miguez@csic.es

† Electronic supplementary information (ESI) available. See DOI: https://doi.org/10.1039/d4tc02362e

‡ Equal contributors.

perovskites.[7] The choice of the A cation has strong implications on the material stability and can further contribute to reduce structural defects acting as charge traps or affect the electronic bandgap edges.[8] Replacing methylammonium (MA) in the proto-typical formulation $MAPbI_3$, employed for record photovoltaic devices in the initial stages of the field, with formamidinium (FA) allowed for a material with enhanced thermal stability and a bandgap close to the optimum value of the Shockley–Queisser limit. This has led to FA-based photovoltaic devices with record efficiencies over the past few years.[9–11] Recently, it has been shown that the Br-containing counterpart $FAPbBr_3$ presents a high phase, moisture and temperature stability,[12] along with high photolumi-nescence (PL) quantum yield (QY), particularly when synthesized in the shape of quantum dots,[13] which has risen the interest in this material for light emitting applications.

When used in solar cells or light emitting diodes (LEDs), semiconductor QDs must be incorporated in the shape of films, in which a certain degree of electronic coupling between the QDs is necessary to allow for charge injection and transport.[14] Among the different routes to fabricate such QD ensembles, ligand-free synthesis within the pores of nanoporous metal oxide matrices has been recently demonstrated as a suitable approach to prepare HP QD films with optical quality and versatility regarding QD size, composition and concentration.[15–20] When deployed as films, the recombination properties of QD undergo pronounced changes and a bulk-like or isolated QD-like behavior is present depending on QD connectivity.[21] The presence of structural defects strongly affects recombination in QD films as photogenerated carriers have access to a larger defect landscape since they can diffuse across many QDs.

In this work we study the role of crystalline defects in charge carrier recombination of ligand-free $FAPbBr_3$ QD films grown within metal oxide nanoporous matrices. In order to evaluate the effect of defects of different nature we explore polymeric encasement, which has been recently shown to act as efficient surface trap passivators,[22] as well as different environmental agents which are known to interact with the defect structure of lead halide perovskites.[23,24] These results are interpreted in the

This journal is © The Royal Society of Chemistry 2024

J. Mater. Chem. C, 2024, **12**, 16683–16690 | **16683**

light of recent literature dealing with the defect structure of FA-based HPs and the role of different trap states in carrier recombination is discussed. We demonstrate how a proper defect passivating strategy can greatly enhance charge diffusion in a QD film, needed for an optimal carrier injection/extraction demanded for optoelectronic applications, and also improved its stability against external radiation. From a fundamental perspective, we provide evidence showing that trap density distribution, rather than QD size distribution, is mostly responsible for the observed variations in emission decay rates present in the QD networks under analysis.

2. Results and discussion

2.1 Bare QD films in an inert N_2 atmosphere

FAPbBr$_3$ QDs were synthetized within the pores of nanoporous SiO$_2$ films (see Fig. 1a) following an already published procedure,[22] detailed in the (ESI†). These samples, labeled FAPbBr$_3$@SiO$_2$, were kept in an air-tight chamber through which different gasses can be flown. Initial measurements were performed in a N_2 atmosphere. By increasing the precursor concentration (C_{prec}), we are able to enhance the connectivity between the QDs embedded within the porous scaffold, since the average inter-QD separation is reduced as we increase their number density.[21] This approach also implies a rise of the average NC size, as it can be seen in Fig. 1b and c, where a reduction in precursor concentration leads to a blueshift in both the absorption edge and PL peak, as expected for NC sizes falling within the quantum confinement regime (estimations for average QD size and separation are given in Table S1 of the ESI†). It is also observed that the average QD separation affects the photoluminescence (PL):[21,22] the higher the connectivity, the lower the PL intensity measured from FAPbBr$_3$@SiO$_2$ samples excited under identical irradiation conditions (see Fig. S2 in the ESI†). Such drop cannot be explained only in terms of a reduced quantum confinement for larger QDs. As QDs get closer, electronic coupling allows charges to diffuse across different QDs, thus expanding the defect landscape they have access to, leading to a reduced PL QY.[21,22] This is further
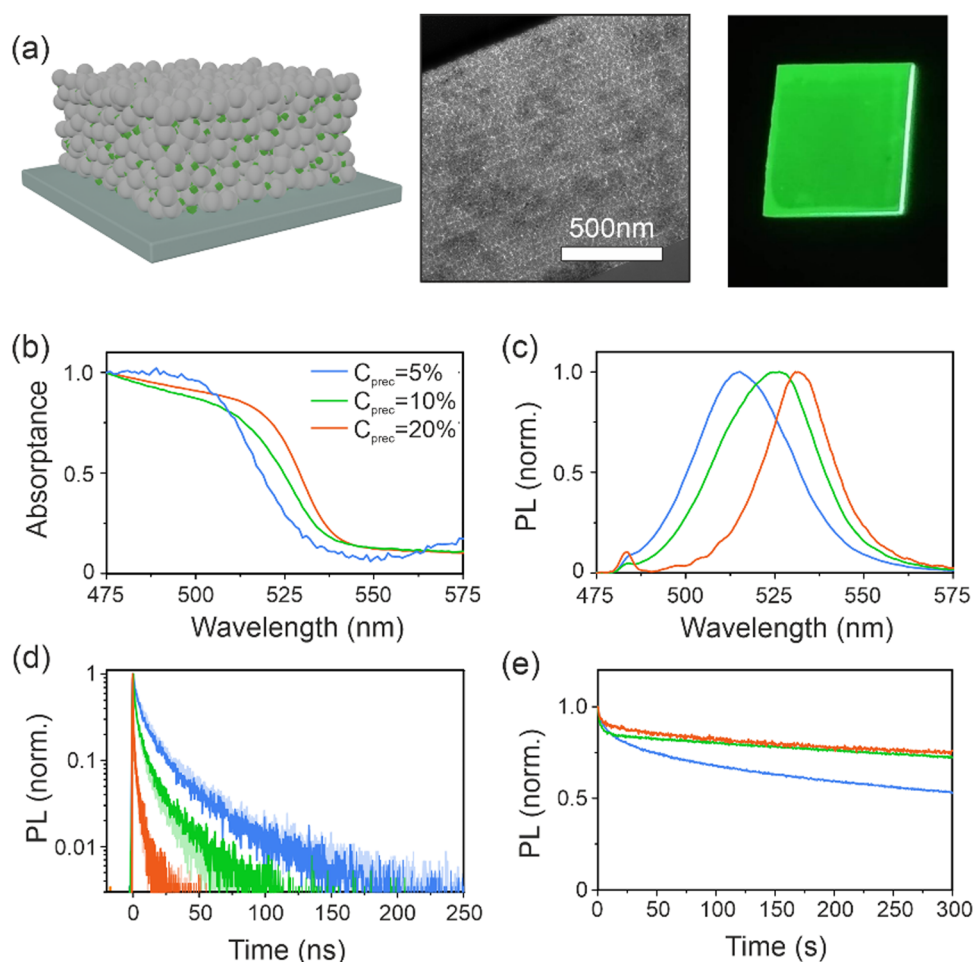

Fig. 1 (a) Scheme of a QD array grown within a SiO$_2$ nanoporous matrix (left), TEM image of a sample infiltrated with a 20% precursor solution (middle) and PL image of a real sample under UV illumination (right). (b) Absorption (normalized at λ = 475 nm), (c) normalized PL, (d) PL decays for high (3 μW, dark curves) and low (30 nW, light curves) and (e) evolution of PL under CW irradiation for samples with different precursor load/interparticle separation. Color code is the same for all four panels: 5%/28 nm (blue), 10%/22 nm (green) and 20%/15 nm (red curve).

reflected in the PL decay of the different samples (Fig. 1d) where a lower PL intensity is accompanied by a faster decay, evidencing additional non-radiative trap-assisted recombination. The measured PL decays were fluence independent for all three samples (Fig. 1d). While this is expected for the lowest precursor concentration, for which a set of isolated QDs is anticipated,[25] the situation for the interconnected QD array should be different, as a bulk-like behavior has been previously reported.[21] This unexpected behavior will be discussed below after analyzing how the defect structure in our samples is modified *via* different treatments.

We next monitored the time evolution of the PL under continuous wave (CW) irradiation over longer time-scales (seconds to minutes) to evaluate the photo-stability of the samples (Fig. 1e). Here an irreversible drop in the PL is observed (Fig. S3, ESI†) indicating the onset of material degradation. Notice that for this and all measurements reported in this work, reversibility of photoinduced changes was evaluated in the same atmosphere as irradiation. This change in emission presents clear differences depending on the sample connectivity (see Fig. S4, ESI†). If we consider the two extreme cases (5 and 20% precursor concentration) we can see that for the sample consisting of a collection of isolated QDs (C_{prec} = 5%), where the PL spectrum is expected to comprise the convolution of spectra from different QDs,[21] emission quenching is more pronounced and affects particularly the red part of the spectrum (Fig. S4a, ESI†), as evidenced by the blueshift of the final emission spectrum compared to the initial one (Fig. S5, ESI†). Such behavior points at non-radiative recombination processes

occurring in the bulk of the larger QDs, which emit in the longer wavelength region. For the case of connected QDs (Fig. S4c, ESI†), PL quenching is less pronounced and does not involve spectral changes. The latter agrees with the fact that, for QD arrays, PL is expected to come from those QDs with smaller bandgap after a carrier diffusion process following the energy landscape of the array. The photostability of FAPbBr$_3$ has been dealt with only recently[26] for macroscopic single crystals where a bulk reversible PL darkening was observed and associated with the perovskite lattice decomposition upon irradiation. In such process, byproducts in gas phase can recombine with other byproducts leading to the recomposition of the lattice. The possible origin of our findings will be further discussed when results for different treatments are dealt with.

To gain further insight into the role of structural defects on both the carrier transport in QD films as well as on the observed photo-instability, we next consider identical samples to the ones discussed above, but with the remaining empty volume of the nanopores infiltrated with poly(methyl methacrylate) (PMMA) after FAPbBr$_3$ QD synthesis (labeled as FAPbBr$_3$@PMMA@SiO$_2$) (see fabrication details in ESI†). This approach, expected to act on surface traps, has been observed in the past to lead to defect passivation and improved PLQY on similar samples.[22] These results are in line with recent *ab initio* studies for FAPbI$_3$, which have shown that, while bulk defects are expected to be more abundant in this material due to a lower defect energy formation,[27] only surface defects occurring for some terminations are expected to introduce deep traps that
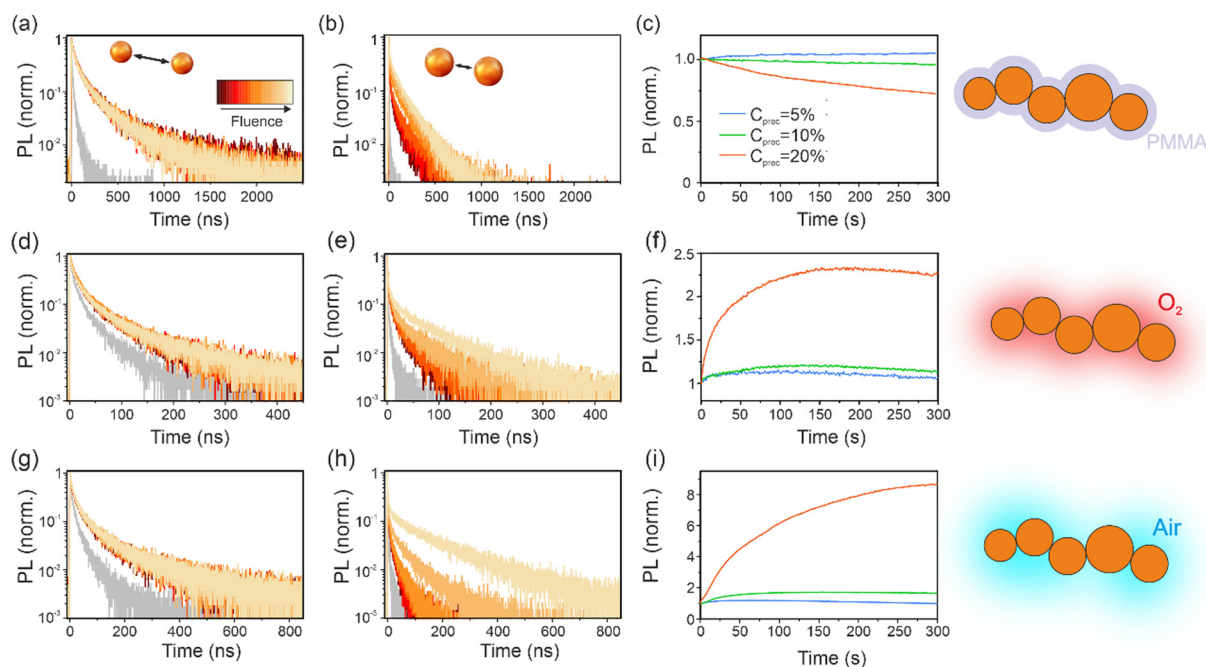

Fig. 2 TRPL for samples with (a) low (C_{prec} = 5%) and (b) high (C_{prec} = 20%) connectivity infiltrated with PMMA. (c) Time evolution of PL under CW irradiation for the three different samples under study: C_{prec} = 5% (blue), C_{prec} = 10% (green) and C_{prec} = 20% (red curve). (d)–(f) and (g)–(i) show identical data for bare samples exposed to O$_2$ and humid air respectively. In all cases, the TRPL data for the same samples in N$_2$ are plotted as grey curves for the sake of comparison.
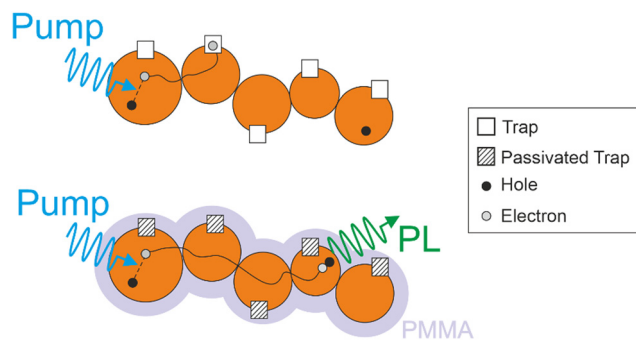
This journal is © The Royal Society of Chemistry 2024

J. Mater. Chem. C, 2024, **12**, 16683–16690 | **16685**

lead to non-radiative recombination paths.[28] For the case of isolated QDs in FAPbBr$_3$@PMMA@SiO$_2$ films with C_{prec} = 5%, an enhanced PL is accompanied by a much longer PL decay evidencing the passivation of deep traps. As before, PL decays are independent of fluence as expected for a collection of isolated QDs (Fig. 2a). For the case of FAPbBr$_3$@PMMA@SiO$_2$ films with larger QD load, where increasingly higher QD inter-connectivity is expected, we observe that not only PL decays become longer than in the presence of N$_2$, but also they show a clear fluence dependence (Fig. 2b). The latter is indicative of a system of interconnected QDs, where recombination dynamics depend on the global population density of charge carriers that can freely move and distribute within the excited area.[21] The stark difference in PL dynamics of FAPbBr$_3$@PMMA@SiO$_2$ samples before and after surface passivation with PMMA high-lights the detrimental role of deep traps in carrier recombina-tion in QD solids. From these data, it becomes apparent that in the presence of a large density of deep traps (as in FAPbBr$_3$@SiO$_2$ samples), carriers generated in one QD recombine non-radiatively at traps either within the QD where they are gener-ated, or at nearby ones where they can diffuse in the case of samples with a higher QD load. In this case, the fact that the carrier can diffuse across QDs increases its defect land-scape, effectively leading to a lower PLQY and, since carriers are trapped before they can diffuse far from its origin, to a negligible effect of the excitation fluence. This situation, which explain the results reported in Fig. S2 (ESI†) for FAPbBr$_3$@SiO$_2$ samples, is represented in the top panel of Scheme 1. On the other hand, as deep traps are passivated, as in FAPbBr$_3$@PMMA@SiO$_2$ samples, carriers can diffuse across many QDs eventually finding an opposite charge to recombine with (bot-tom panel in Scheme 1) and presenting a fluence dependence on recombination that reflects its dependence on global popu-lation density.

Trap passivation in FAPbBr$_3$@PMMA@SiO$_2$ samples not only influences emission properties but also photostability. Now, samples having the lower QD loads and thus expected to consist of a collection of isolated QDs do not show any variation in PL, evidencing the absence of structural changes

Scheme 1 Proposed picture for carrier recombination and the role of deep traps. (top) For bare QD films carriers generated in a given QD rapidly recombine non-radiatively at a trap within the same or an adjacent QD. (bottom) Upon passivation of the surface traps, carriers can diffuse across the QD film before recombining.

taking place (see Fig. 2c). The fact that irreversible degradation is now absent for this sample indicates that surface traps, beyond acting as deep traps leading to the quenching of PL, also represent seed points where degradation is triggered. For the case of the samples with higher precursor load where QD interconnectivity is expected (C_{prec} = 20%) we now observe a photo-induced PL darkening that is reversible when CW irradiation is removed (see Fig. S6, ESI†). Two types of mechan-isms have been reported for reversible photodarkening in HPs. A decomposition of the HP lattice into its precursors and further formation of gaseous byproducts was invoked in ref. 26 as the process leading to reversible darkening of FAPbBr$_3$ single crystals when excitation is performed in the bulk and byproducts cannot scape the crystal. If this mechanism was behind our observations, PL darkening should be observed for all QD films regardless of their load. On the other hand, Motti and co-workers proposed[29] the formation of I$_2$ upon annihila-tion of halide-related Frenkel pairs as a possible origin for PL quenching. This would explain the present results in the event that halide defects could migrate across different QDs in our interconnected samples. Br$_2$ forming as a result of the annihi-lation of Frenkel pairs could not escape the film due to the presence of the PMMA film and the process could be reversed upon removing the CW irradiation.

Next, we consider the surrounding atmosphere as a treatment with potential to modify the defect landscape in FAPbBr$_3$@SiO$_2$ samples. The role of the environment on HP photophysics and stability has been extensively studied over the past decade. There is nowadays a consensus that certain gases can strongly modify the defect landscape in LHP at the expense of reducing material stability so that a compromise must be attained if one wants to employ this approach to optimize their optoelectronic properties.[30,31] In this work we have explored the role of O$_2$ and moisture. We first exposed our sample to a continuous flow of dry O$_2$ (<3 ppm background humidity according to the provider, Linde) for 5 minutes prior to study their optical properties. Time resolved photoluminescence (TRPL) data shows a slight slowing in the PL decays for all samples under study (Fig. 2d and e). This is likely related with the interaction of O$_2$ with a certain population of deep traps, as evidenced by the fact that TRPL becomes again fluence dependent for the highly connected sample. This interaction takes place *via* weak binding of O$_2$ to FAPbBr$_3$ (physisorption) as the effect is rapidly reversed upon restoring a N$_2$ atmosphere.

More evident changes appear when the effect of O$_2$ is combined with that of CW irradiation and we monitor the sample PL (Fig. 2f). Here we can observe that samples with small connectivity barely experience any change in their PL but highly connected samples undergo a >2 fold enhancement, pointing to the photoinduced interaction of deep traps with this reactive atmosphere. As with the case of samples infiltrated with PMMA, no spectral changes were observed for the highly connected samples (Fig. S7, ESI†). While reports on the inter-action of O$_2$ with FAPbBr$_3$ are lacking, recent evidence showing emission changes of other MA-based HP may hold the key to explain the present results. In particular, a photoinduced PL rise in the presence of O$_2$ has been previously reported[32–38] and

16686 | *J. Mater. Chem. C*, 2024, **12**, 16683–16690

This journal is © The Royal Society of Chemistry 2024

associated with the formation of superoxide species[35–38] which may interact with surface halide vacancies which, as in the present case, act as deep traps. This effect is reversible over times longer than those needed for activation following a two-step process with different time scales of seconds and tens of minutes (see Fig. S8, ESI†).

Finally, $FAPbBr_3$@SiO_2 samples were exposed to humid air to explore the combined action of O_2 and moisture. H_2O is known to accelerate phase instability for $FAPbI_3$ while, for the case of $FAPbBr_3$, is known to have little effect on its stability.[12] Further, the combination of H_2O and O_2 has been recently reported to lead to accelerated degradation in iodide based mixed Cs-FA HPs.[39] As in the case of exposure to pure O_2, the TRPL of all samples undergo a slowing of the PL dynamics (Fig. 2g), although more pronounced. For the more connected QDs, a significantly stronger fluence dependence is observed (Fig. 2h), indicating a larger population of defects interacting with H_2O and O_2 than with O_2 alone. Again, irradiating with CW light in the presence of humid air leads to more dramatic changes in emission, as shown in Fig. 2i. Here a small (ca. 10–30%) PL enhancement is observed for the case of isolated QDs while connected ones undergo a remarkable 10-fold enhancement. Resorting to previous reports for MA-based HP, the combined action of H_2O and light has been suggested to improve the HP emission according to two mechanisms. Brenes and co-workers proposed the partial dissolution of the HP lattice at the surface, leading to the formation of an amorphous film that could act as a passivator.[36,38] Alternatively, other oxide species can form at the HP surface, namely peroxide[37] and hydrogen peroxide.[40] These species can further react with uncoordinated lead, in different charge states, present at the HP surface which can be oxidized into lead oxide.[37,40] Both processes would lead to the irreversible passivation of traps and thus a different mechanism is expected in our case as, while much longer recovery times are observed than when using only O_2, (see Fig. S9, ESI†) our sample returns to its initial low PL state. Hence, further work will be needed in order to unveil the photoinduced processes involving water that lead to such efficient interaction of atmospheric agents with traps in $FAPbBr_3$ QDs.

For the case of $FAPbBr_3$@SiO_2 films exposed to non-inert atmospheres, while the population of traps interacting with the surrounding atmosphere is expected to be the same for all different samples, the photoinduced PL enhancement is more pronounced for the case of connected QDs. The reason behind this observation is the stronger effect of traps on the sample emission for connected QD arrays (see Scheme 1), where a larger defect landscape arises as a consequence of carriers being able to diffuse across several QDs. To evaluate and quantify the role of the different treatments, we consider the C_{prec} = 5% samples, i.e. those having the lowest connectivity, where fluence does not play a role in the emission. We compare the PL decay under different atmospheres as representative of the weight of non-radiative processes. To extract a parameter for comparison we fit the TRPL to a lognormal distribution of decays, $\rho(\Gamma)$ (see Fig. 3a for the $FAPbBr_3$@PMMA@SiO_2 sample, and Fig. S10 (ESI†) for $FAPbBr_3$@SiO_2 exposed to different atmospheres). As previously reported,[21] the mode of the distribution (Γ_m) represents an average value of the decay rate of the distribution of QDs. The width of this distribution will be affected by the size dispersion but could also be influenced by the defect distribution in different QD. From the comparison of all Γ_T it becomes clear that the treatment that more efficiently de-activates deep traps is that of PMMA (Fig. 3b), further highlighting the detrimental role of surface defects in this material. Additional information can be extracted from a comparison of the actual decay rate distribution for QD films in N_2 and with the different treatments (see Fig. 3c). The average value of the decay rate distribution Γ_T comprises a radiative (Γ_R) and a non-radiative (Γ_{NR}) component. While the former is assumed to be identical for all samples, the latter depends on the defect landscape as:

$$\Gamma_{NR} = \sigma_{trap} v_{th} N_T$$

Hence the non-radiative recombination is directly affected by the number of trap sites in the system, (N_T) their capture cross section (σ_{trap}) and the thermal velocity of the free charge carriers (v_{th}), the latter remaining unchanged for the different treatments. The reduction of the number of trap sites can be explained as halide related defects interact with environmental gas molecules, while a change in σ_{trap} can be assigned to a change in the energy level of a trap state, such as the one predicted for interstitial iodide in the presence of O_2.[41] To shed
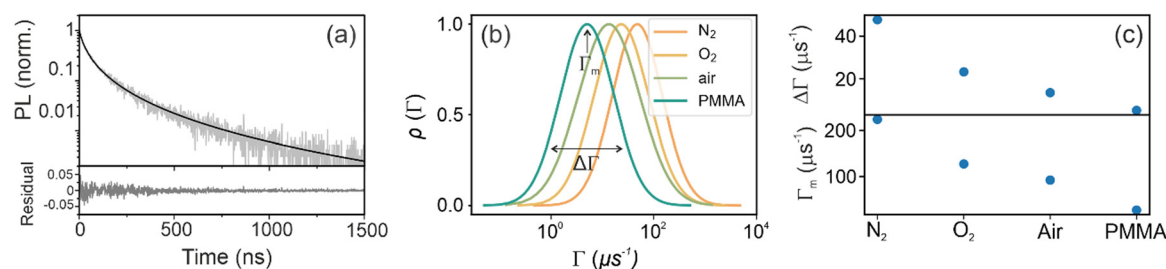

Fig. 3 (a) TRPL for a sample with low connectivity (C_{prec} = 5%) infiltrated with PMMA. Grey (black) curve represents experimental data (fit to a lognormal distribution of decay rates). Bottom panel shows the residual of the fit. (b) Lognormal distribution of decay rates from fit of experimental data for samples exposed to different treatments, as indicated in the horizontal axis. (c) Width (top) and average value (bottom panel) of the distributions of the C_{prec} = 5% sample under the different treatments.

This journal is © The Royal Society of Chemistry 2024

J. Mater. Chem. C, 2024, **12**, 16683–16690 | **16687**

more light into the exact origin of the reduction in Γ_{NR}, the distribution of recombination rates is analyzed in the following. Here it can be seen that adding the polymer as a passivating agent not only reduces the average decay rate, evidencing the reduction of non-radiative recombination paths, but also homogenizes the PL dynamics of the QD distribution as its width is reduced by an order of magnitude (Fig. 3c). This latter fact further evidences that trap density distribution, rather than size distribution, is mostly responsible for the observed variation in decay rates in the present QD films.

The distribution of decay rates can be associated to both the non-radiative (Γ_{NR}) and radiative (Γ_R) components, where non-radiative components are expected to show both larger decay times and a broader distribution of decay times. As the different treatments (atmosphere and PMMA) are acting on the sample, a reduction of the decay rate distribution is observed (Fig. 3c). The continuous decrease of both the average values of the distribution and its width is observed as surface defects interact with one of the abovementioned agents. Since both parameters decrease in the same monotonic way, the global reduction in decay rates can be solely assigned to the reduction in the number of trap states. A significant change in the distribution of defect states would involve a more drastic change in the width $\Delta\Gamma$, rather than in the mean rate Γ_m. Further, an assignment of the broad distribution to a size and energy dispersion due to the heterogeneity of the crystals is discarded, as in this case, $\Delta\Gamma$ and Γ_m would not follow identical dynamics.

3. Conclusions

In summary, we have explored the role of defects in charge recombination for HP QD films using ligand-free QDs fabricated within the pores of silicon oxide matrices. The use of different treatments evidences that surface traps are a main source of non-radiative recombination in FA-based HP and its presence constitutes a burden for carrier transport in QD films. Thus, a proper passivation approach represents an efficient avenue for avoiding this issue and improving the performance of devices containing these materials. Further, surface traps have also been shown to represent a source of instability leading to irreversible material degradation in the absence of appropriate passivation. Finally, we have presented the first evidence of photo-induced PL activation in FA-based HP as a consequence of the combined action of irradiation and exposure to reactive atmospheres. This latter effect is mainly related with defect reactivity at the HP surface and thus previous reports dealing with larger samples could not observe it.

Data availability

The data underlying this study are openly available in the Digital CSIC repository: http://hdl.handle.net/10261/368936. The codes used to fit the TRPL data are provided at https://github.com/Multifunctional-Optical-Materials-Group.

Conflicts of interest

There are no conflicts to declare.

References

1 A. K. Jena, A. Kulkarni and T. Miyasaka, Halide perovskite photovoltaics: background, status, and future prospects, *Chem. Rev.*, 2019, **119**, 3036–3103.

2 K. Ji, M. Anaya, A. Abfalterer and S. D. Stranks, Halide Perovskite Light-Emitting Diode Technologies, *Adv. Opt. Mater.*, 2021, **9**, 2002128.

3 L. Lei, Q. Dong, K. Gundogdu and F. So, Metal halide perovskites for laser applications, *Adv. Funct. Mater.*, 2021, **31**, 2010144.

4 H. Huang, B. Pradhan, J. Hofkens, M. B. J. Roeffaers and J. A. Steele, Solar-driven metal halide perovskite photocatalysis: design, stability, and performance, *ACS Energy Lett.*, 2020, **5**, 1107–1123.

5 H. Wei and J. Huang, Halide lead perovskites for ionizing radiation detection, *Nat. Commun.*, 2019, **10**, 1066.

6 H. Lin, C. Zhou, Y. Tian, T. Siegrist and B. Ma, Low-dimensional organometal halide perovskites, *ACS Energy Lett.*, 2018, **3**, 54–62.

7 L. A. Muscarella and E. M. Hutter, Halide double-perovskite semiconductors beyond photovoltaics, *ACS Energy Lett.*, 2022, **7**, 2128–2135.

8 J. Lee, S. Tan, S. Seok, Y. Yang and N. Park, Rethinking the A cation in halide perovskites, *Science*, 2022, **375**, eabj1186.

9 M. Jeong, I. W. Choi, E. M. Go, Y. Cho, M. Kim, B. Lee, S. Jeong, Y. Jo, H. W. Choi, J. Lee, J. H. Bae, S. K. Kwak, D. S. Kim and C. Yang, Stable perovskite solar cells with efficiency exceeding 24.8% and 0.3–V voltage loss, *Science*, 2020, **369**, 1615–1620.

10 J. Jeong, M. Kim, J. Seo, H. Lu, P. Ahlawat, A. Mishra, Y. Yang, M. A. Hope, F. T. Eickemeyer, M. Kim, Y. J. Yoon, I. W. Choi, B. P. Darwich, S. J. Choi, Y. Jo, J. H. Lee, B. Walker, S. M. Zakeeruddin, L. Emsley, U. Rothlisberger, A. Hagfeldt, D. S. Kim, M. Grätzel and J. Y. Kim, Pseudo-halide anion engineering for α-fapbi₃ perovskite solar cells, *Nature*, 2021, **592**, 381–385.

11 H. Min, D. Y. Lee, J. Kim, G. Kim, K. S. Lee, J. Kim, M. J. Paik, Y. K. Kim, K. S. Kim, M. G. Kim, T. J. Shin and

16688 | *J. Mater. Chem. C*, 2024, **12**, 16683–16690

This journal is © The Royal Society of Chemistry 2024

S. Il Seok, Perovskite Solar cells with atomically coherent interlayers on SnO_2 electrodes, *Nature*, 2021, **598**, 444–450.

12 P. Raval, R. M. Kennard, E. S. Vasileiadou, C. J. Dahlman, I. Spanopoulos, M. L. Chabinyc, M. Kanatzidis and G. Manjunatha Reddy, Understanding instability in formamidinium lead halide perovskites: kinetics of transformative reactions at grain and subgrain boundaries, *ACS Energy Lett.*, 2022, **7**, 1534–1543.

13 H. Bhatia, B. Ghosh and E. Debroye, Colloidal FAPbBr$_3$ perovskite nanocrystals for light emission: what's going On?, *J. Mater. Chem. C*, 2022, **10**, 13437–13461.

14 Y. Zhang, G. Wu, F. Liu, C. Ding, Z. Zou and Q. Shen, Photoexcited Carrier Dynamics in Colloidal Quantum Dot Solar Cells: Insights into Individual Quantum Dots, Quantum Dot Solid Films and Devices, *Chem. Soc. Rev.*, 2020, **49**, 49–84.

15 D. N. Dirin, L. Protesescu, D. Trummer, I. V. Kochetygov, S. Yakunin, F. Krumeich, N. P. Stadie and M. V. Kovalenko, Harnessing defect-tolerance at the nanoscale: highly luminescent lead halide perovskite nanocrystals in mesoporous silica matrixes, *Nano Lett.*, 2016, **16**, 5866–5874.

16 M. Anaya, A. Rubino, T. C. Rojas, J. F. Galisteo-López, M. E. Calvo and H. Míguez, Strong Quantum Confinement and Fast Photoemission Activation in $CH_3NH_3PbI_3$ Perovskite Nanocrystals Grown within Periodically Mesostructured Films. Adv, *Opt. Mater.*, 2017, **5**, 1601087.

17 V. Malgras, S. Tominaka, J. W. Ryan, J. Henzie, T. Takei, K. Ohara and Y. Yamauchi, Observation of Quantum Confinement in Monodisperse Methylammonium Lead Halide Perovskite Nanocrystals Embedded in Mesoporous Silica, *J. Am. Chem. Soc.*, 2016, **138**, 13874–13881.

18 S. Demchyshyn, J. M. Roemer, H. Groi, H. Heilbrunner, C. Ulbricht, D. Apaydin, A. Böhm, U. Rütt, F. Bertram, G. Hesser, M. C. Scharber, N. S. Sariciftci, B. Nickel, S. Bauer, E. D. Głowacki and M. Kaltenbrunner, Confining Metal-halide Perovskites in Nanoporous Thin Films, *Sci. Adv.*, 2017, **3**, e1700738.

19 V. Malgras, J. Henzie, T. Takei and Y. Yamauchi, Stable Blue Luminescent CsPbBr3 Perovskite Nanocrystals Confined in Mesoporous Thin Films, *Angew. Chem., Int. Ed.*, 2018, **57**, 8881–8885.

20 A. Rubino, L. Caliò, A. García-Bennett, M. E. Calvo and H. Míguez, Mesoporous Matrices as Hosts for Metal Halide Perovskite Nanocrystals, *Adv. Opt. Mater.*, 2020, **8**, 1901868.

21 D. O. Tiede, C. Romero-Pérez, K. A. Koch, B. Ucer, M. E. Calvo, A. R. K. Kandada, J. F. Galisteo-López and H. Míguez, Effect of Connectivity on the Carrier Transport and Recombination Dynamics of Perovskite Quantum-Dot Networks, *ACS Nano*, 2024, **18**, 2325–2334.

22 C. Romero-Pérez, N. Fernández-Delgado, M. Herrera-Collado, M. E. Calvo and H. Míguez, Ultrapure Green High Photoluminescence Quantum Yield from FAPbBr$_3$ Nanocrystals Embedded in Transparent Porous Films, *Chem. Mater.*, 2023, **35**(14), 5541–5549.

23 Z. Andaji-Garmaroudi, M. Anaya, A. J. Pearson and S. D. Stranks, Photobrightening in Lead Halide Perovskites: Observations, Mechanisms, and Future Potential, *Adv. Energy Mater.*, 2020, **10**, 1903109.

24 J. F. Galisteo-López, M. E. Calvo and H. Míguez, The Complex Interplay of Lead Halide Perovskites with their Surroundings. Adv, *Opt. Mater.*, 2021, **9**, 2100133.

25 Q. A. Akkerman, T. P. Nguyen, S. C. Boehme, F. Montanarella, D. N. Dirin, P. Wechsler, F. Beiglbök, G. Rainò, R. Erni, C. Katan, J. Even and M. V. Kovalenko, Controlling the nucleation and growth kinetics of lead halide perovskite quantum dots, *Science*, 2022, **377**, 1406–1412.

26 D. R. Ceratti, Y. Rakita, L. Cremonesi, R. Tenne, V. Kalchenko, M. Elbaum, D. Oron, M. A. C. Potenza, G. Hodes and D. Cahen, Self healing inside APbBr$_3$ halide perovskite crystals, *Adv. Mater.*, 2018, **30**, 1706273.

27 S. Tan, I. Yavuz, M. H. Weber, T. Huang, C.-H. Chen, R. Wang, H.-C. Wang, J. H. Ko, S. Nuryyeva and J. Xue, *et al.*, Shallow Iodine Defects Accelerate the Degradation of α-phase Formamidinium Perovskite, *Joule*, 2020, **4**, 2426–2442.

28 S. M. Oner, E. Sezen, M. S. Yordanli, E. Karakoc, C. Deger and I. Yavuz, Surface Defect Formation and Passivation in Formamidinium Lead Triiodide (FAPbI$_3$) Perovskite Solar Cell Absorbers, *J. Phys. Chem. Lett.*, 2022, **13**, 324–330.

29 S. G. Motti, D. Meggiolaro, A. J. Barker, E. Mosconi, C. A. R. Perini, J. M. Ball, M. Gandini, M. Kim, F. De Angelis and A. Petrozza, Controlling competing photochemical reactions stabilizes perovskite solar cells, *Nat. Photonics*, 2019, **13**, 532–539.

30 Z. Andaji-Garmaroudi, M. Anaya, A. J. Pearson and S. D. Stranks, Photobrightening in Lead Halide Perovskites: Observations, Mechanisms, and Future Potential, *Adv. Energy Mater.*, 2020, **10**, 1903109.

31 J. F. Galisteo-López, M. E. Calvo and H. Míguez, The Complex Interplay of Lead Halide Perovskites with their Surroundings, *Adv. Opt. Mater.*, 2021, **9**, 2100133.

32 J. F. Galisteo-Lopez, M. Anaya, M. E. Calvo and H. Miguez, Environmental Effects on the Photophysics of Organic–Inorganic Halide Perovskites, *J. Phys. Chem. Lett.*, 2015, **6**, 2200–2205.

33 Y. Tian, M. Peter, E. Unger, M. Abdellah, K. Zheng, T. Pullerits, A. Yartsev, V. Sundström and I. G. Scheblykin, Mechanistic Insights into Perovskite Photoluminescence Enhancement: Light Curing with Oxygen can Boost Yield Thousandfold, *Phys. Chem. Chem. Phys.*, 2015, **17**, 24978–24987.

34 S. G. Motti, M. Gandini, A. J. Barker, J. M. Ball, A. R. Srimath Kandada and A. Petrozza, Photoinduced Emissive Trap States in Lead Halide Perovskite Semiconductors, *ACS Energy Lett.*, 2016, **1**, 726–730.

35 X. Feng, H. Su, Y. Wu, H. Wu, J. Xie, X. Liu, J. Fan, J. Dai and Z. He, Photon-generated Carriers Excite Superoxide Species Inducing Long-term Photoluminescence Enhancement of MAPbI$_3$ Perovskite Single Crystals, *J. Mater. Chem. A*, 2017, **5**(24), 12048–12053.

36 R. Brenes, D. Guo, A. Osherov, N. K. Noel, C. Eames, E. M. Hutter, S. K. Pathak, F. Niroui, R. H. Friend and M. S. Islam, Metal Halide Perovskite Polycrystalline Films

This journal is © The Royal Society of Chemistry 2024

J. Mater. Chem. C, 2024, **12**, 16683–16690 | **16689**

Exhibiting Properties of Single Crystals, *Joule*, 2017, **1**, 155–167.

37 M. Anaya, J. F. Galisteo-López, M. E. Calvo, J. P. Espinós and H. Míguez, Origin of Light-Induced Photophysical Effects in Organic Metal Halide Perovskites in the Presence of Oxygen, *J. Phys. Chem. Lett.*, 2018, **9**(14), 3891–3896.

38 R. Brenes, C. Eames, V. Bulović, M. S. Islam and S. D. Stranks, The Impact of Atmosphere on the Local Luminescence Properties of Metal Halide Perovskite Grains, *Adv. Mater.*, 2018, **30**, 1706208.

39 J. Hidalgo, W. Kaiser, Y. An, R. Li, Z. Oh, A. F. Castro-Méndez, D. K. LaFollette, S. Kim, B. Lai, J. Breternitz, S. Schorr, C. A. R. Perini, E. Mosconi, F. De Angelis and J. P. Correa-Baena, Synergistic Role of Water and Oxygen Leads to Degradation in Formamidinium-Based Halide Perovskites, *J. Am. Chem. Soc.*, 2023, **145**, 24549–24557.

40 J. S. W. Godding, J. A. Ramadan, Y.-H. Lin, K. Schutt, H. J. Snaith and B. Wenger, Oxidative Passivation of Metal Halide Perovskites, *Joule*, 2019, **3**(11), 2716–2731.

41 D. Meggiolaro, E. Mosconi and F. De Angelis, Mechanism of Reversible Trap Passivation by Molecular Oxygen in Lead-Halide Perovskites, *ACS Energy Lett.*, 2017, **2**, 2794–2798.

16690 | *J. Mater. Chem. C*, 2024, **12**, 16683–16690

This journal is © The Royal Society of Chemistry 2024